Edinburgh Research Explorer

Benchmarking large scale GPR experiments on railway ballast

Benchmarking Large Scale GPR Experiments on Railway Ballast

Dr R De Bold, G O'Connor, JP Morrissey, Professor MC Forde (corresponding author)
University of Edinburgh
School of Engineering
AGB Building
The Kings Buildings
Edinburgh EH9 3JL, UK
Tel: +44 131 650 5721
m.forde@ed.ac.uk

KEYWORDS

Railway, track bed, maintenance, GPR, ballast, testing, spent, analysis, benchmarking

ABSTRACT

The overall aim of this project was to relate Ground Penetrating Radar (GPR) to a ballast fouling index (FI).

Laboratory research aimed at characterising the electromagnetic properties has enabled researchers worldwide to determine ballast thickness using impulse Ground Penetrating Radar (GPR) - based upon derived values of the relative electrical permittivity or dielectric constant. In this paper, a series of GPR experiments, following on from these laboratory experiments, were undertaken on a full scale track bed using a range of bowtie antennas from 500MHz to 2.6GHz. The key innovation reported is the use of scatter analyses of the GPR waveforms, featuring area, axis crossing and inflexion point analyses. These scatter analyses were then used to predict the Ionescu ballast Fouling Index. A correlation coefficient greater than 0.9 was obtained by using a 500MHz bowtie antenna in the parallel orientation in conjunction with a scan area analysis.

1 INTRODUCTION

The "green agenda" combined with highway congestion has accelerated the demand for increased capacity for both freight and passenger travel on the world's railways. The distance travelled by UK national rail passengers has increased from 28.7 billion passenger-kilometres in 1994 (UK Department of Statistics, 2007) to 58.0 billion passenger-kilometres in 2012 (UK Department of Transport, 2013). A similar growth trend in the use of rail can be seen in the United States where rail usage has increased from 1,752 billion tonne-kilometres in 1994 (Association of American Railroads, 2006) to 2,469 billion tonne-kilometres in 2011 (International Union of Railways, 2011); however, in this case the growth is mainly in the freight haulage sector.

Ballasted track is the most widely used track bed material on the railways. Ballasted track bed supports stresses imposed upon the rails and in conjunction with the sleepers ("ties" in the US), maintains their correct position. The ballast structure, featuring large voids, provides for necessary drainage of water and fouling material. Over time, ballast deteriorates through a process of degradation, where the particles mechanically abrade, or weather, and change shape; or, through fouling, where fine particles accumulate in the void structure. Subsoil intrusion is a major source of fouling. Deteriorated ballast is defined as "spent" and fails to provide the drainage and mechanical functions required. Spent ballast can also be described as "fouled".

Historically the traditional methods of inspecting ballast are by (a) visual inspection – which is subjective; (b) use of trial pits – which is expensive and intrusive, requiring track possession. More recently ground penetrating radar (GPR) has been used, albeit in an embryonic format.

Against the above comments, the objectives of this paper are to: -

1. Review the current concept of GPR testing of railway track bed ballast;

2. Review the knowledge base of the dielectric properties of railway ballast; and,

3. Present new methods of analysis for assessing ballast fouling of railway track bed using Ground Penetrating radar (GPR).

2   PRINCIPLES OF GPR

Ground Penetrating Radar (GPR) is a geophysical imaging method based on measuring reflected electromagnetic (EM) waves transmitted in the form of radar pulses in the microwave band of the radio spectrum (UHF/VHF frequencies). A transmitting di-pole antenna radiates EM pulses into the ground and a receiving di-pole antenna measures variations in the reflected signal in a time domain profile. Reflections occur as the signal moves through heterogeneous material interfaces between two media of differing dielectric properties.

Small-scale heterogeneities, or changes in dielectric impedance, generate weak or undetectable responses but attenuate energy as the signal passes due to scattering (Annan, 2008). Scattering losses are frequency dependant – they increase as the frequency increases. GPR has become well established for testing of concrete (Bungey & Millard, 1993) (Soutsos, Bungey, Millard, Shaw, & Patterson, 2001) (Forde & McCavitt, 1993).

These interface reflections give responses from which the underground structural profile can be inferred. This can be seen in Figure 1, where a diagram of a railway profile (left hand side of the diagram) is matched against a typical radar line scan response profile (middle), and the combination of several scans produce an underground radar profile (right). Due to its layered nature, GPR is ideally suited for railway applications, with the possibility of data being collected at high speeds (Clark, Gordon, & Forde, 2004).
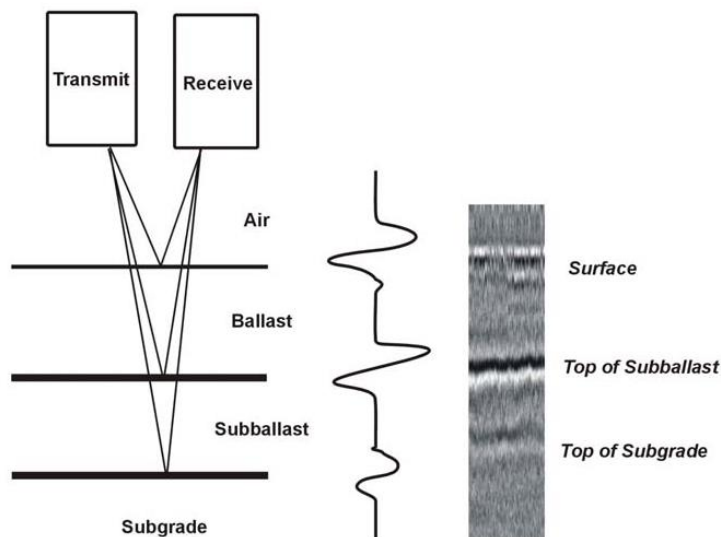
Figure 1 Generation of a GPR profile

2.1   GPR in Railways

Much of the work in the field of using GPR in railways has concentrated on monitoring the layering of the subsurface; there has been little work in attempting to determine track condition. GPR has been found to be useful in determining the layering profile of track substructure and areas of high moisture content within it; such areas produce stronger reflections (Dolphin, Beatty, & Tanzi, 1978) and water pockets can also be detected (Zarembski, 1988).

One field study found that by making the broad assumption that the velocity of signal propagation in ballast is 1.4×10^8 m/s, that the thickness of the ballast layer could be calculated to an accuracy of 3cm; and some determination of the extent of subsoil penetration into the ballast layer could also be identified (Hugenschmidt, Railway track inspection using GPR, 2000). Al-Qadi et al (2010) have focused work on optimising the layout of antennas for higher quality data collection.

Historically, spent ballast could only easily be identified visually at the same time as track failure, or, before this, through disruptive and intrusive means. This was thus a reactive regime. However, over the previous decade, ongoing research into GPR testing has changed this: -

- Investigation of the imaging attributes of railway track formation using ground penetrating radar (Jack & Jackson, 1998);

- Development of ballast inspection using ground penetrating radar (Hugenschmidt, Ballast inspection using ground penetrating radar, 1999);

- Investigation of railway track bed deterioration using GPR (Gallagher G. P., 1999);

- Evaluation of the electromagnetic properties of railway ballast using GPR (Gallagher G. P., Leiper, Clark, & Forde, 2000);

- Analysis of electromagnetic properties of railway ballast (Clark, Gillespie, Kemp, McCann, & Forde, 2001); and,

- Investigation of issues regarding high-speed non-invasive monitoring of railway track bed (Clark, Gordon, & Forde, 2004).

Complementary work was undertaken elsewhere by others: -

- Using a falling weight deflectometer on railway ballast to determine stiffness (Sharpe & Collop, 1998);

Consequently, GPR can be used for a qualitative first indication of ballast condition, and also facilitates the better targeting of intrusive and disruptive site investigations (Brough, Stirling, Ghataora, & Madelin, 2003). It has also been proposed that GPR can be used as a method for track bed quality control by providing continuous ballast depth data (Sharpe, 2000).

Previous research visually compared ground penetrating radar response signals of variously fouled ballast on a specially constructed 10m long full-scale track bed (Gallagher G. P., Investigation of Railway Trackbed Deterioration using Ground Penetrating Radar, 1999). This work proved effective, as the EM velocity through clean ballast is higher than that through spent ballast. The reason being that clean ballast contains significant air voids and the EM waves travel through air at a significantly higher velocity.

Subsequent laboratory research sought to relate the GPR response of ballast to its relative electrical permittivity or "dielectric constant" (Clark, Gillespie, Kemp, McCann, & Forde, 2001) (Clark, Gordon, & Forde, Issues over high-speed non-invasive monitoring of railway trackbed, 2004).

3   LABORATORY GPR TESTING OF BALLAST

In order to be able to quantify ballast fouling from field data, a series of carefully controlled experiments were undertaken on railway ballast.

The objectives of the laboratory work were to determine if ballast condition, i.e., clean or spent, could be determined from the calculated relative electrical permittivity or "dielectric constant", ε_r; and whether the 500MHz or 900MHz GPR antenna was more suitable at this task.

For the laboratory experiments, a large brick tank structure was constructed in which the ballast could be placed easily to a suitable depth (Figure 5).
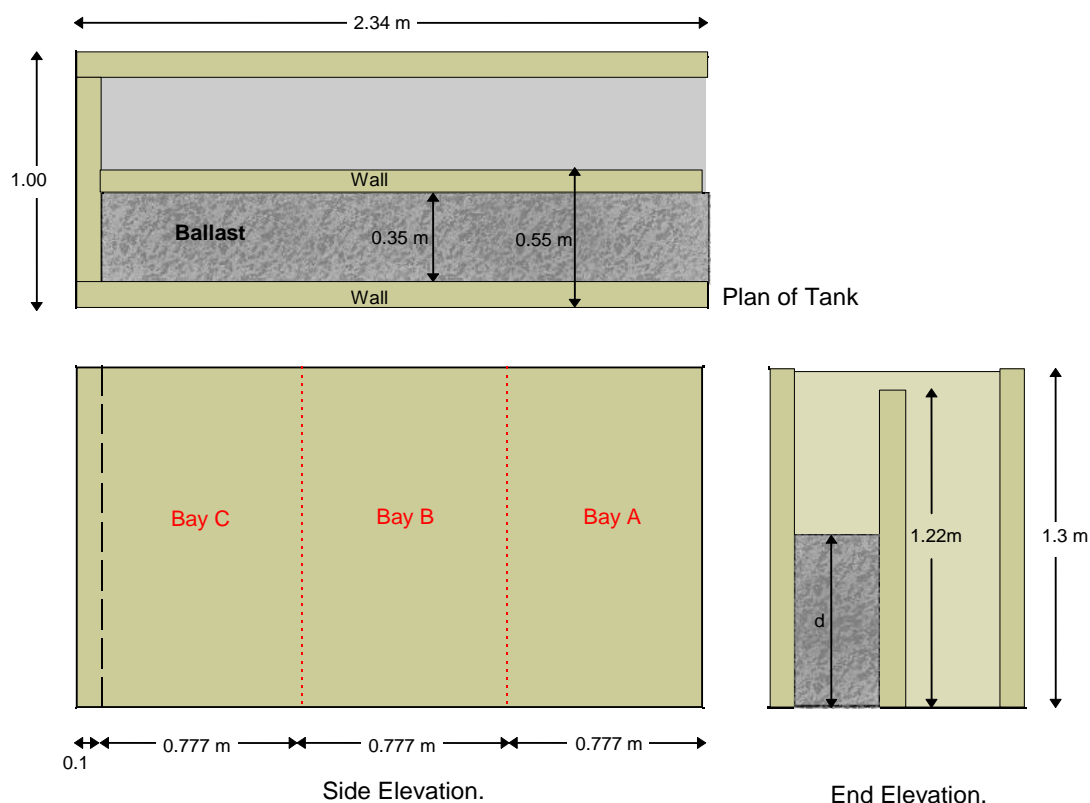
Figure 2 Tank dimensions (Clark M. , 2001)

The experiment was undertaken twice: once with unused clean ballast and once with spent ballast at the end of its life span recovered from a railway track bed. The placing and compaction of the ballast was intended to mimic real track conditions, as can be seen in Figure 3: -
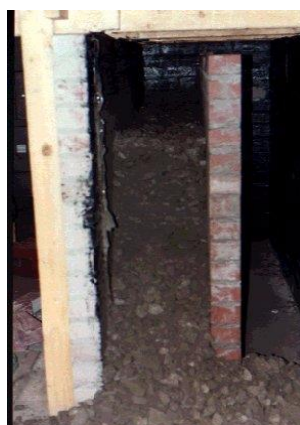
Figure 3 Tank containing 0.75m of spent ballast (Clark M. , 2001)

The experiment was undertaken by dragging each radar antenna along the surface of each ballast type, as can be seen in Figure 4: -
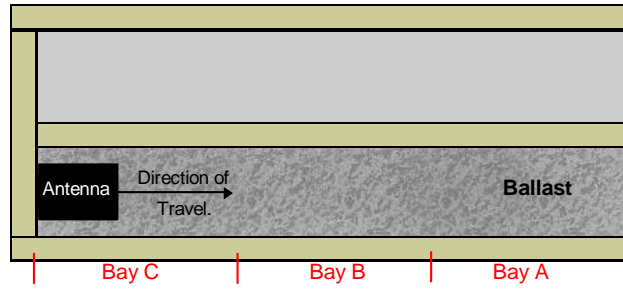
Figure 4 Plan view of test rig (Clark M. , 2001)

The ballast was assumed to be a low loss material, and, therefore, the simplified velocity equation of electromagnetic waves in a dielectric medium for low-loss materials (materials having a small dissipation of electric or electromagnetic power) (Daniels, Gunton, & Scott, 1988) was suitable to be used to determine the dielectric constant and velocity of wave propagation for the different types of ballast tested: -

$$v = \frac{c}{\sqrt{\varepsilon_r}}$$

Where, v = velocity of propagation;

c = speed of light (3×10^8 m/s); and,

ε_r = dielectric constant of the medium.

Therefore, the depth of the reflecting interface is calculated from the measured two way travel time, i.e., the time there and back, and the speed of the electromagnetic wave: -

$$t_r = \frac{2d}{v} = \frac{2d\sqrt{\varepsilon_r}}{c}$$

Where, t_r = two way travel time; and,

d = depth to interface.

It was found that the dielectric constant for the spent ballast under dry or wet conditions was greater than that for the clean ballast. These results for the dielectric constant were also comparable with other results for ballast (Sussmann, 1999), as can be seen in Table 1: -

Material (* by volume)	Source	ε_r	velocity (m/s)	Density (Mg/m³)

Air	(Clark M. , 2001)	1	3.00×10^8	
Dry Clean Ballast	(Clark M. , 2001)	3.0	1.73×10^8	1.6
Wet Clean Ballast (5% water*)	(Clark M. , 2001)	3.5	1.60×10^8	
Dry Clean	(Sussmann, 1999)	3.6	1.58×10^8	
Dry Spent	(Sussmann, 1999)	3.7	1.56×10^8	
Moist Clean	(Sussmann, 1999)	4	1.50×10^8	
Dry Spent Ballast	(Clark M. , 2001)	4.3	1.45×10^8	1.8
Moist Spent	(Sussmann, 1999)	5.1	1.32×10^8	
Wet Spent	(Sussmann, 1999)	7.2	1.12×10^8	
Wet Spent Ballast (5% water*)	(Clark M. , 2001)	7.8	1.07×10^8	
Saturated Clean Ballast	(Clark M. , 2001)	26.9	0.48×10^8	
Saturated Spent Ballast	(Clark M. , 2001)	38.5	0.58×10^8	
Water	(Clark M. , 2001)	81	0.33×10^8	1

Table 1 List of electromagnetic properties for various materials (Clark M. , 2001)

These variations in dielectric constant values were attributed to: -

- Clean ballast having a greater volume of air voids, which lowers the average dielectric constant of the medium (and therefore increases the transmission velocity);
- Water increasing the average dielectric constant of the medium; (and therefore reducing the transmission velocity); and,
- Spent ballast with its greater fines content can hold more water than clean ballast, thus "wet spent" ballast has a higher dielectric constant than "wet clean" ballast (and therefore an even lower transmission velocity).

The radar plots of the ballast using the 900MHz and 500MHz antennas can be seen in Figure 5 and Figure 6: -
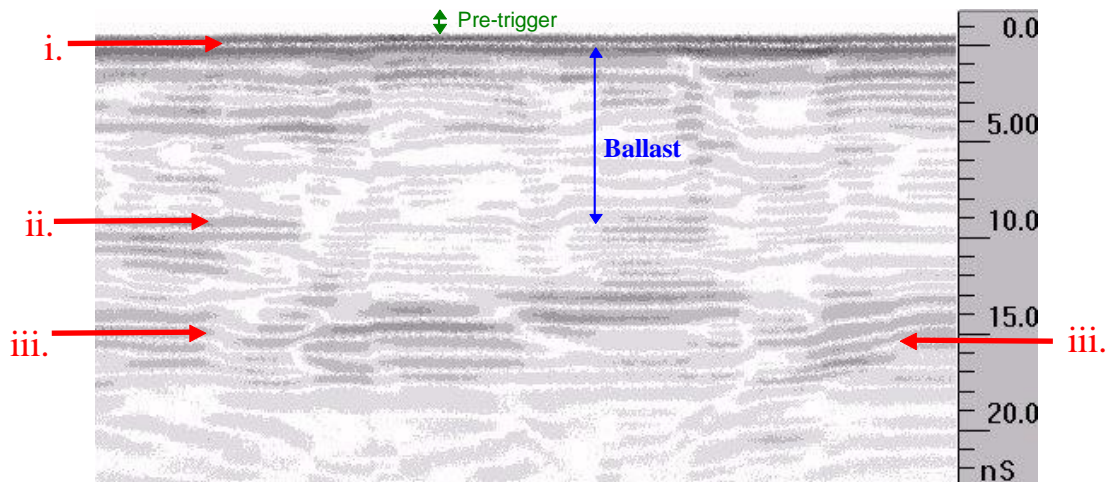
Figure 5 Subsurface profile of 1m of spent ballast – 900MHz antenna (Clark M. , 2001)
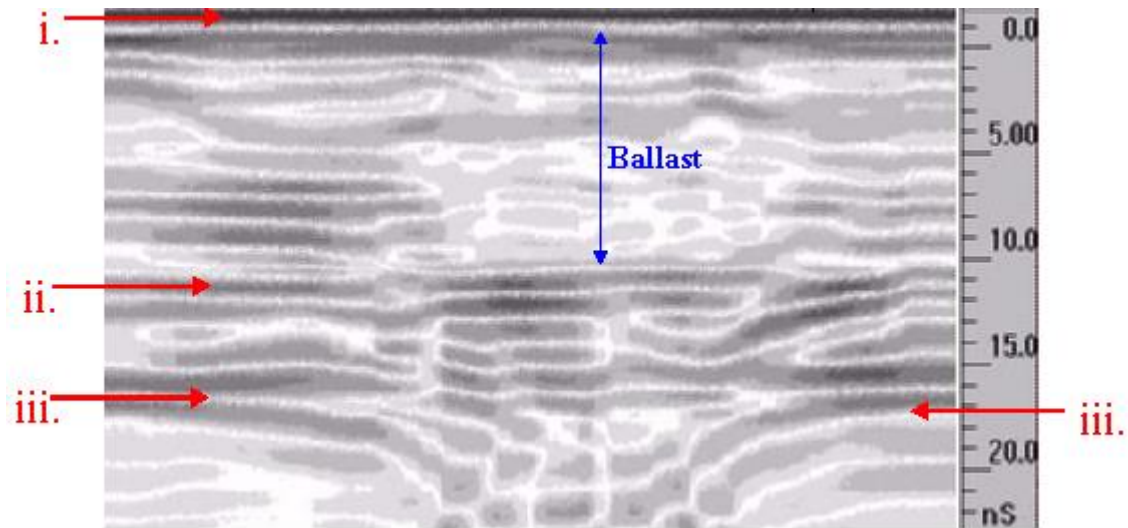
Figure 6 Subsurface profile of 1m of spent ballast – 500MHz antenna (Clark M. , 2001)

Analyses of the plots show where the: -

   i.   Electromagnetic wave enters the ballast surface;
   ii.   Wave reflects from base of tank; and,
   iii.   Diagonal "swipe signatures" are caused by reflections from the tank walls.

The 500MHz antenna had a greater depth penetration and showed the ground reflection from the laboratory concrete floor more clearly than the 900MHz antenna. The 500MHz antenna also had a lesser resolution than the 900MHz antenna resulting in less reflection, and less clutter, from the individual ballast particles, which also resulted in more pronounced swipe signatures.

4   FULL SCALE RAILWAY TRACKBED

A 10m long track was built to British Rail Standard BR1203 (July 1985, amended May 1988) at the University of Edinburgh, King's Buildings campus, Edinburgh, UK. It is of uniform construction and materials, except that there was the deliberate addition of fines in some parts to induce its "spent" nature (Figure 7).
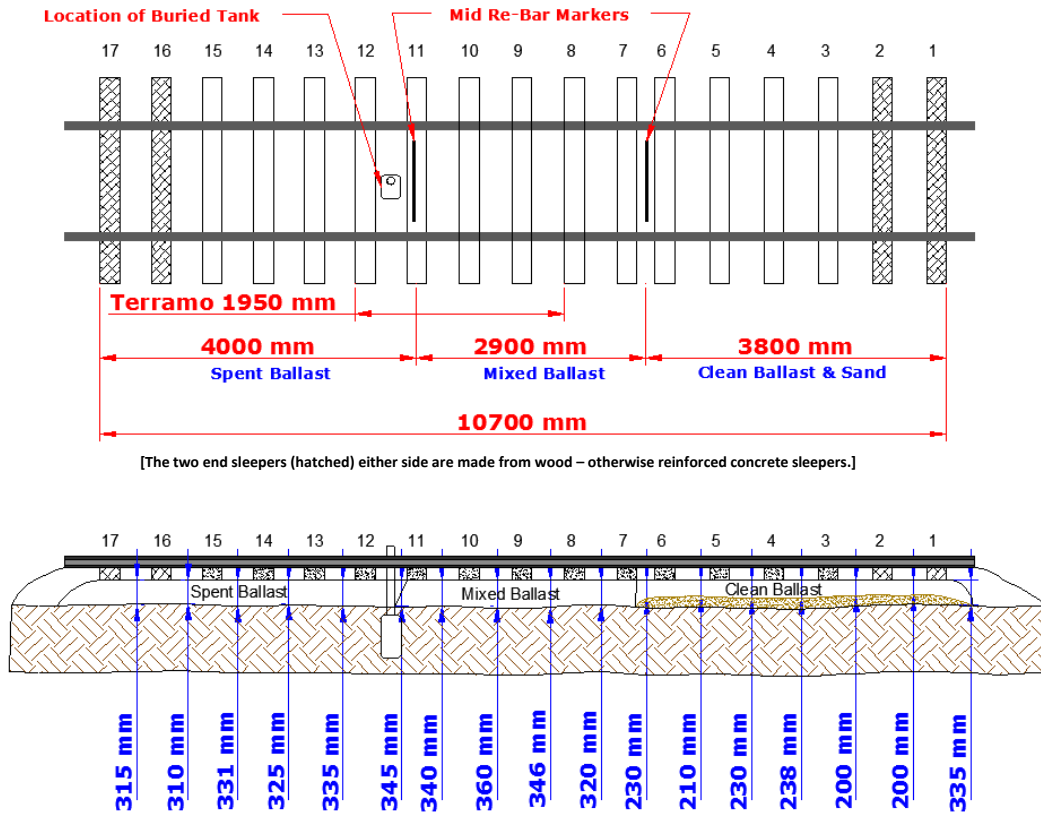
Figure 7 Full-scale track bed facility (modified Clark, 2001)

5 GPR WAVEFORM ANALYSIS

Previous GPR research on the full-scale track bed (Gallagher G. , Leiper, Williamson, Clark, & Forde, 1999) found that on studying the time-amplitude plot of a single radar pulse reflection, it could be seen that where the ballast was "spent" the signal plot featured "scattering" between the surface reflection response and the ballast-formation layer interface reflection; where the ballast was not spent, there was no "scattering" (Figure 8).
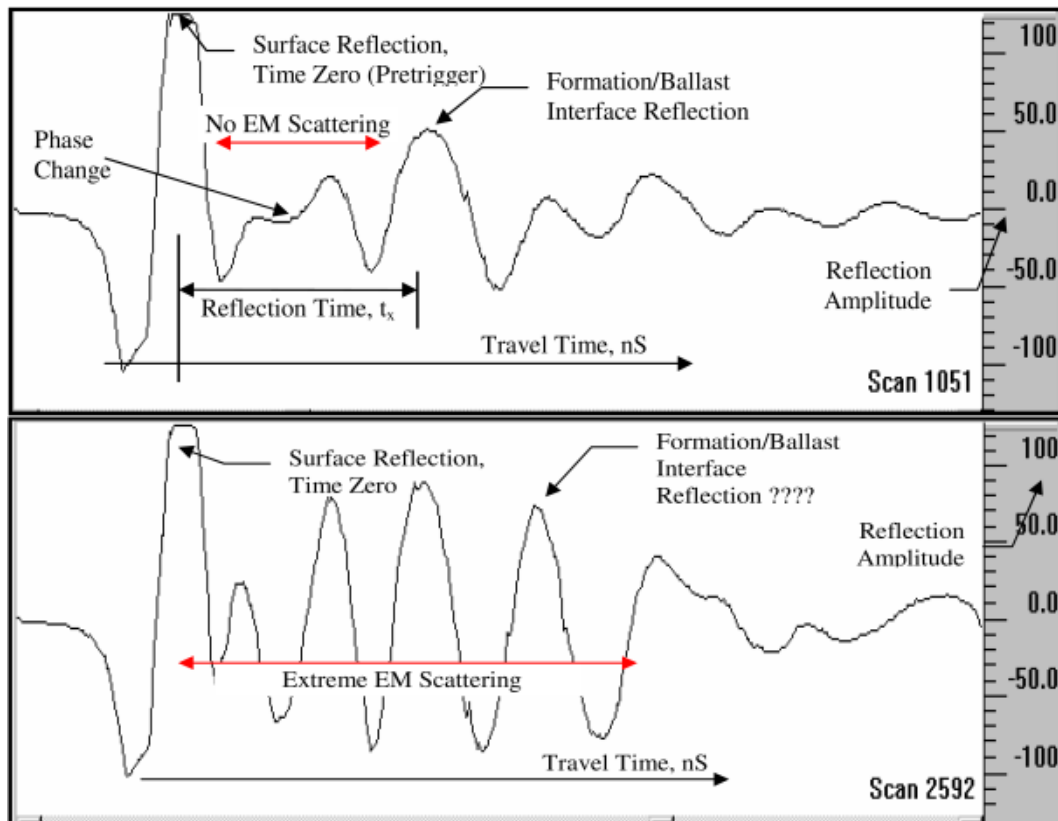
Figure 8 Example of 500MHz signal plot through clean (top) and spent ballast (bottom) (Gallagher G. P., Investigation of Railway Trackbed Deterioration using Ground Penetrating Radar, 1999)

Two antennas were used: 900MHz and 500MHz. The 500MHz antenna demonstrated increased power and the lower centre frequency resulted in a greater depth penetration over the 900MHz. The resolution was significantly lower (approximately halved, consequent with the reduction in frequency). However, the reflection times through the same media were similar. None of the antennas managed to produce reflections through the sleepers.

The 500MHz and 900MHz signals through the clean ballast gave no EM scattering, and gave a clear formation reflection. Through the mixed ballast, there was increased EM scattering, a less clear formation reflection, and a reduced propagation velocity consequent with a greater dielectric constant. Through the spent ballast there was extreme EM scattering making the formation reflection indistinguishable, and a further reduced propagation velocity. The 900MHz signals demonstrated greater scattering than the 500MHz signals through the same material.

The differences in results were attributed to the spent ballast having a greater fines content with consequently fewer air voids, poorer drainage efficiency, and, thus, greater moisture content due to moisture retention from soil suction. Loss of voids (with a very low dielectric value) and replacement with moist fines (with a significantly higher dielectric value) resulted in the increased scattering and attenuation.

The experiments were repeated several times over one year in different weather conditions. It was found that the clean ballast results varied by 5% to 7%; the spent ballast results varied up to 25%. Ballast-saturation tests carried out in the laboratory (Clark, Gillespie, Kemp, McCann, & Forde, 2001) determined that the greater variability of the spent ballast was due to its ability to hold water due to soil suction, or capillarity, and become saturated due to rain; the clean ballast is more free-draining and less affected by rain.

This research demonstrated that railway ballast could be fingerprinted using GPR.

5.1 Scattering Analysis and Fouling Detection

With the laboratory experiments, there was no attempt to analyse the waveform of the reflected signals, only its velocity. The presence of the edge effects would make waveform analysis unreliable, although such edge effects are unavoidable in a contained laboratory calibration experiment. Thus, large scale field experiments were required for the analysis of waveforms (avoiding edge effects).

The concept of analysing the GPR waveform to determine the quality of ballast has been undertaken before. At the Transportation Technology Center, Inc. (TTCI) in Pueblo, Colorado, analysis of the waveform taken from horn antennas (Roberts, Al-Qadi, Tutumluer, Boyle, & Sussmann, 2006) were used to detect ballast fouling.

At TTCI, they found that with the use of 2GHz horn antennas - that clean ballast gave a more scattered response than fouled ballast (Al-Qadi, Xie, & Roberts, Scattering analysis of ground-penetrating radar data to quantify railroad, 2008).

In contrast to traditional GPR data analysis, in which individual reflections are charted, the 2GHz horn antenna data from the ballast was processed to generate a representative scattering amplitude envelope, i.e., a running average between peak signal responses that showed the average scattering amplitude versus depth.

A change in the size of the envelope was determined to indicate a change in ballast condition. A "gain restoration curve", which was empirically derived from the amplitude correction required to achieve constant amplitude versus arrival time from data obtained over a section of thick, clean ballast, was, presumably, applied to discount the effects of attenuation.

Radar signals through the clean ballast scattered due to the void spaces present in clean ballast – but not in spent ballast where they had been in-filled with fouling material. The fouled ballast was more homogenous in its structure – hence the signal scattered less.

This rationale was presented in subsequent research (Roberts, Al-Qadi, Tutumluer, Boyle, & Rudy, 2006), which stated that because spent ballast has a "finer, well-graded particle size with fewer air voids" that "the clean ballast near the surface generates a significant scattering pattern, while the scattering pattern generated by the fouled ballast at the bottom is insignificant because the air voids in fouled ballast are much smaller than the signal wavelength". The above research at TTCI was conducted on ballast composed of a clean layer of ballast, over a mixed layer of ballast, over a spent layer of ballast, all of varying thicknesses using horn antennas. This is in contrast to the work reported herein, where GPR research used bowtie antennas on one homogeneous layer of ballast.

Given that the metric used in the TTCI research is the "scattering amplitude envelope" and that this would be expected to diminish with depth due to attenuation, the "scattering amplitude envelope" method, relies on discerning changes in the amplitude and relating that to changes in the ballast condition through empirically derived calibrations. It is not a true numerical analysis of the GPR waveform. Therefore, an alternative measurement of "scattering" that is not attenuation related would be attractive to investigate.

5.2 Track Bed Analysis

Since construction, the test track has likely undergone physical changes that could be attributed to weather conditions and experimentation. A full investigation of the ballast condition by means of particle size distribution (PSD) analysis was undertaken to enable quantification of the relationship between GPR data and ballast condition.

The PSD results were analysed to determine the fouling index for each crib (the space between two sleepers). There are two methods for calculating ballast deterioration: Selig & Waters (1994) and Ionescu (2004). Ionescu adheres to Australian standards that are similar to the material parameters used in British track bed construction; consequently, the Ionescu method was used: -

$$F_I = P_{0.075} + P_{14}$$

Where:

F_I = Fouling index

$P_{0.075}$ = % passing 0.075mm sieve

P_{14} = % passing the 14mm sieve

The categories of fouling developed by Selig & Waters (1994), as can be seen in Table 2, were used in conjunction with the derived fouling index formula to determine the test track condition. However, the threshold for "clean" was slightly changed to 1.5% (from 1%) so that for the purposes of analysis, Cribs 1 to 6, including Crib 11, are "Clean"; Cribs 7 to 10 are "Moderately Fouled"; and, Cribs 12 to 16, are "Fouled".

Category	Fouling Index (F_I)		
Clean	<1.5		
Moderately Clean	1.5	-	10
Moderately Fouled	10	-	20
Fouled	20	-	40
Highly Fouled	>40		

Table 2 Categories of fouling (modified Selig & Waters, 1994)

These categories broadly coincide with the placement of the clean, mixed, and spent ballast, except for Crib 11, which is "clean" when it should at least be "Moderately Fouled". However, as per Figure 7, Crib 11 features the addition of a submerged tank for a previous experiment and it is speculated that the act of digging out the ballast of this crib, placing the tank, and then refilling the crib had the effect of "cleaning" the ballast of it fines.

The categories were used in conjunction with the Ionescu fouling index formula to determine the condition of the test track (Table 3 and Figure 9): -

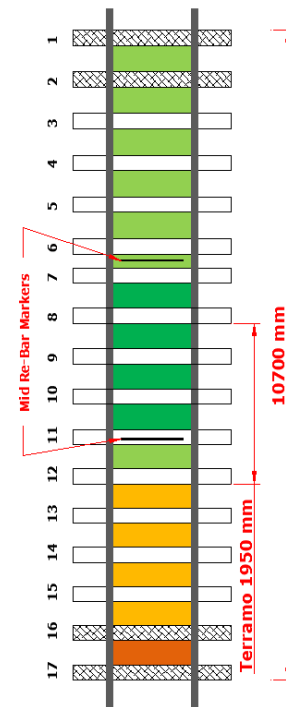| Crib No.	F_I	Category
1	0.90%	Clean
2	1.05%	Clean
3	0.77%	Clean
4	0.84%	Clean
5	1.37%	Clean
6	0.79%	Clean
7	3.00%	Moderately Clean
8	4.80%	Moderately Clean
9	7.12%	Moderately Clean
10	7.20%	Moderately Clean
11	0.99%	Clean
12	13.79%	Moderately Fouled
13	17.45%	Moderately Fouled
14	10.79%	Moderately Fouled
15	11.70%	Moderately Fouled
16	20.47%	Fouled

Table 3 Ballast fouling index   **Figure 9 Ballast condition schematic**

A limitation of such a fouling index is that although the degree of fouling is related to the spentness of the ballast, it is only a function of spentness. This is because fouling index is solely a description of the fines content of a particular ballast sample but spentness is a description of a collection of various other variables such as fines content, drainage efficiency, and surface texture (Parker, 1997).

5.3 Large Scale Track Bed Waveform Analyses

5.3.1 *Objectives*

The objectives of this experimental work were to develop a method of analysing the incidents of scatter, rather than amplitude of the scatter, using a range of different frequency antennas.

5.3.2 *Experimental Procedure*

Gallagher (1999), defined the increased scattering through a visual inspection of a signal plot, where the increased numbers of large peaks were a result of the EM wave being scattered by the smaller particles of the spent ballast. It has been stated that the signal from ballast can be assumed to be a random signal and that statistical analysis would be a more suitable method of analysis (Roberts, Al-Qadi, Tutumluer, Boyle, & Rudy, 2006).

5.3.3 *Data Collection*

The track was scanned with a range of GSSI antennas of different frequencies: 500MHz, 900MHz, 1.0GHz, 1.6GHz, and 2.6GHz.

The higher frequency bowtie antennas may not be suitable for detecting faults or anomalies in ballast and may be more suited to tasks such as locating objects in concrete. Their inclusion was intended to reveal trends in the analysis across the range of frequencies.

All data was collected using either a trolley or with a survey wheel designed to locate the antennas and measure distances travelled. The data was recorded without any gain settings distorting the collected data.

The scanning procedure started with the antennas moving from Sleeper 1 to Sleeper 17. Given that bowtie antennas transmit from one side of their casing and receive at the other, this was undertaken twice with the antenna in perpendicular then parallel orientation (Figure 10).
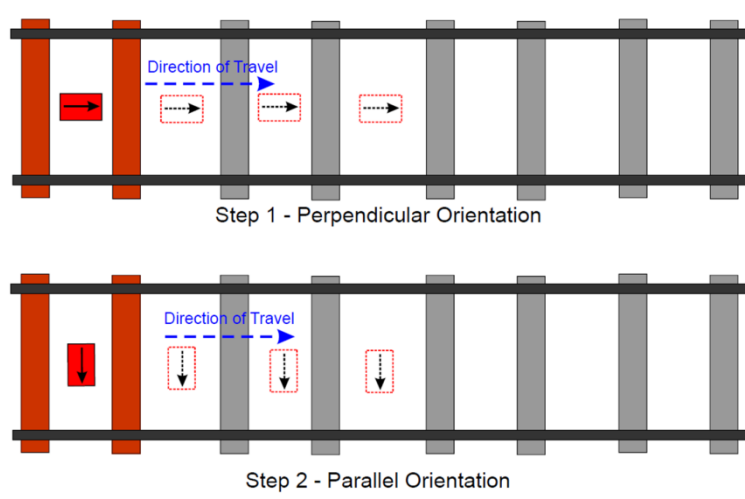
Figure 10 Data collection method

A scan rate of 200scans/m was used, resulting in over 2000 scans for each run of the test track; although, 100scans/m was used for the 500MHz and 900MHz. Each scan was composed of 512 samples, giving over one million data values per run.

5.4   Data Analysis

The raw numerical data for each run was imported into an individual spreadsheet and contour plots of the radar data were produced and these were used to visually isolate the "cribs" (Figure 11) – those areas between the sleepers where the ballast is on the surface creating Crib 1 to Crib 16.
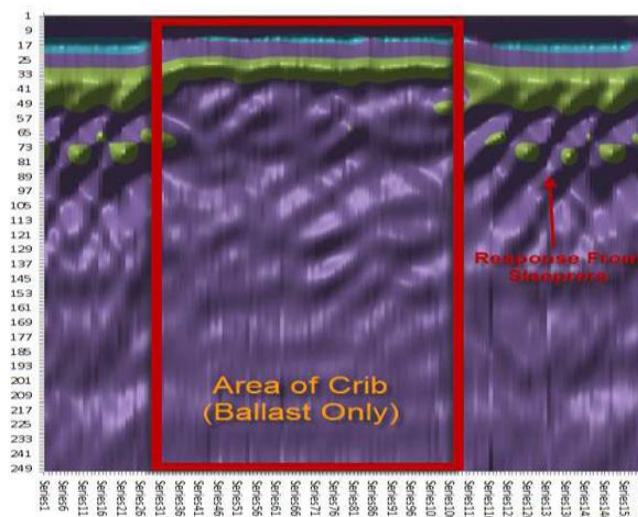
Figure 11 Example of 3D contour plot used for crib isolation for 2.6GHz data

In order to calculate the incidents of scatter for each crib, three metrics were devised: -

Scan area	A numerical integration of a scan response to determine its "area" – the greater the magnitude of the responses, the greater the area.
Axis crossings	The number of times the scan response crosses the zero amplitude axis – the more interfaces encountered by the signal, the more axis crossings.
Inflection points	The number of times the gradient of the scan response changes through zero – the more interfaces, the more inflection points.

5.4.1   Scan Area Analysis

For each scan, the average signal value was calculated. This value was taken as the zero amplitude axis for that scan and a simple trapezoidal rule was utilised to integrate some or all of the 512 sample values of each scan (Figure 12) to determine the "area" of the scan as highlighted in yellow.

Figure 12 Scan area for typical clean response (left) and spent response (right)

5.4.2   Axis Crossings Analysis

For each scan, the average signal value was calculated. This was taken as the zero amplitude axis for that scan and the number of times that the signal crossed the average value was counted. Extrapolating from Gallagher's findings from signal responses through spent ballast (Gallagher G. P., Investigation of Railway Trackbed Deterioration using Ground Penetrating Radar, 1999), it was anticipated that the more a signal is scattered, the more it should cross the axis.

A simple algorithm counted the number of crossing points. For any sample value that was between a sample value greater than the average scan value and a sample value lower than the average scan value, an axis-crossing was counted (Figure 13).
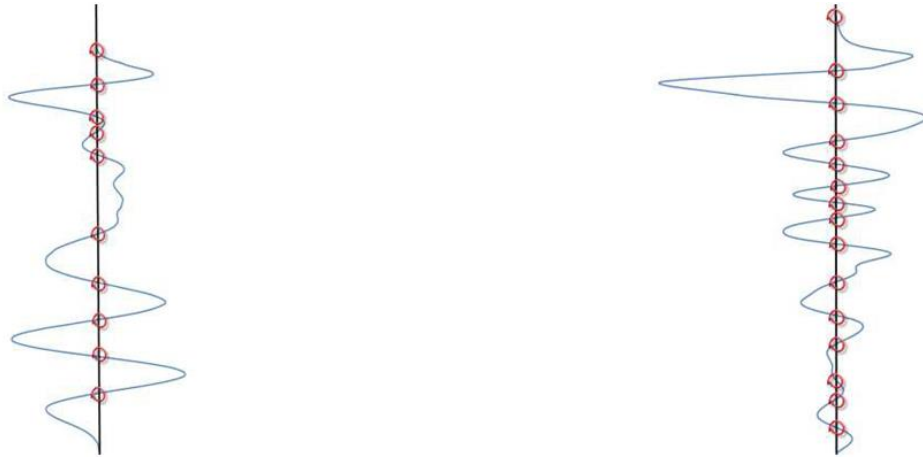
Figure 13 Axis crossings for typical clean response (left) and spent response (right)

5.4.3   Inflection Points Analysis

For each scan, the number of inflection points was counted. Similar to crossing points, it was anticipated that the more scattered a response, the more inflection points it should have.

The number of inflection points was calculated by using a variation of the algorithm used to count the crossing points. For any sample value that was between two greater value samples or between two lower value samples, an inflection point was counted (Figure 14). This method did not require the location of the zero amplitude axis.

Figure 14 Inflection points for typical clean response (left) and spent response (right)

5.4.4   Time Range

Given the different frequencies of each antenna, different depths of penetration were achieved and recorded. It was noted at which of the 512 samples that the ground surface occurred and where the response was visually considered to have become noise dominant. Therefore, for the analysis three different time ranges were used: -

Full time range: All 512 samples collected were analysed.

Common time range: Only 5ns of data below the initial ground reflection was analysed in order to limit analysis to ballast responses only.

> **Proportional time range:** By evaluating the skin depth of each antenna and the original range it was set to detect, a ratio of the relative penetration of each antenna was calculated.

6   RESULTS & DISCUSSION

By using the Scan Area Analysis, the Axis Crossings Analysis, and the Inflection Points Analysis metrics, the amount of signal scattering was identified. The data was analysed using three different approaches to determining which sample time ranges to use: the full 512 samples, a reduced common range (5ns), and a time range proportional to penetration.

6.1   Full Time Range Results

The average results of the scattering analysis for each type of ballast using the full time range of the scan are listed in Table 4. The highest values for each section of analysis (area, crossings, and inflections) are highlighted in red and the lowest in green.

Antenna	Orientation	Range (ns)	Area Of Scan			Axis Crossings			Inflection Points		
			Clean	Mod. Clean	Mod. Fouled, Fouled	Clean	Mod. Clean	Mod. Fouled, Fouled	Clean	Mod. Clean	Mod. Fouled, Fouled
500 MHz	Perp.	23	1269272	1820730	2088340	15.57	16.02	16.99	17.50	18.12	19.31
	Parallel	23	1179536	1568375	2059104	15.31	16.02	16.70	17.81	17.28	18.62
900 MHz	Perp.	20	696421	987018	1235757	27.69	23.48	24.05	45.92	37.05	36.17
	Parallel	20	817121	1077727	1555518	26.25	23.67	23.91	46.10	38.22	35.31
1.0 GHz	Perp.	20	703692	952372	974882	29.58	29.06	28.55	33.59	32.20	31.07
	Parallel	20	972730	1210584	1204123	26.67	25.77	26.97	32.79	31.68	31.89
1.6 GHz	Perp.	20	430589	416034	407551	21.86	19.86	19.41	56.49	52.07	54.22
	Parallel	20	383307	426471	423533	19.63	15.95	16.79	54.81	51.50	53.42
2.6 GHz	Perp.	10	333581	339728	338602	20.59	20.30	20.23	16.44	15.16	14.98
	Parallel	10	376546	394878	385945	20.27	19.98	19.56	23.48	22.48	22.04

Table 4 Results of scattering analysis for full time range

6.2   Full Time Range Scan Area Analysis

It can be seen that the clean ballast has the smallest area in most cases with the spent or mixed ballast having the largest areas. This trend is very strong at the lower frequencies under 1GHz; this correlates with Gallagher et al. 1999 (Gallagher G. , Leiper, Williamson, Clark, & Forde, 1999).

6.3   Full Time Range Axis Crossings Analysis

Similar to the area analysis, there is a difference in behaviour between high and low frequency antennas. With antennas of 900MHz or over, the clean ballast features more axis crossings than the spent ballast. Below 900MHz, the behaviour is the reverse with the spent ballast having more axis crossings than the clean.

6.4   Full Time Range Inflection Points Analysis

The results are very similar to the axis crossing points analysis with the same behaviour occurring. Again, the 900MHz antenna appears to be the point at which the behaviour changes, with almost 20% more inflection points.

6.5 Common Time Range Results

The average results of the scattering analysis for each type of ballast using the common time range of the scan are listed in Table 5. The highest values for each section of analysis (area, crossings, and inflections) are highlighted in red and the lowest in green.

Antenna	Orientation	Range (ns)	Scan Area			Axis Crossings			Inflection Points		
			Clean	Mod. Clean	Mod. Fouled, Fouled	Clean	Mod. Clean	Mod. Fouled, Fouled	Clean	Mod. Clean	Mod. Fouled, Fouled
500 MHz	Perp.	5	519361	649110	493665	3.95	3.87	3.78	4.47	4.47	5.32
	Parallel	5	495875	585394	531113	3.38	3.96	4.26	4.77	4.40	5.25
900 MHz	Perp.	5	222113	242224	258231	6.91	5.58	6.72	9.14	7.91	8.44
	Parallel	5	201378	242690	253223	6.45	5.40	6.74	8.89	7.51	8.36
1.0 GHz	Perp.	5	149771	187753	190682	7.85	8.08	7.74	9.22	8.97	8.55
	Parallel	5	179378	218713	201614	6.84	7.24	7.21	8.81	8.75	8.76
1.6 GHz	Perp.	5	382593	362212	352233	9.89	9.73	9.50	11.04	11.30	10.86
	Parallel	5	353525	412695	403925	8.47	8.29	8.05	10.28	9.23	9.59
2.6 GHz	Perp.	5	299528	302294	300923	10.63	10.65	10.75	14.42	13.22	12.96
	Parallel	5	331064	347733	339890	10.55	10.50	10.36	14.32	13.55	13.05

Table 5 Results of scattering analysis for common range

6.6 Common Time Range Scan Area Analysis

The trend in results of the area analysis are similar in trend to those of the full time range; the clean ballast generally has the smaller area, although, the clear difference between clean and fouled ballast at frequencies below 900MHz is no longer present.

6.7 Common Time Range Axis Crossings Analysis

Unlike the full range analysis, the trend in the results is of a more random nature.

6.8 Common Time Range Inflection Points Analysis

The trend in the results is also similar to those of the full time range. The 900MHz antenna contains significantly more inflection points for clean ballast whilst the 500MHz antenna has more inflection points in spent ballast. All of the high frequency antennas, with the exception of the 1.6GHz perpendicular antenna, have more inflection points in clean ballast than in spent ballast.

6.9 Proportional Time Range Results

The average results of the scattering analysis for each type of ballast using the proportional time range of the scans are listed in Table 6. Each antenna was analysed in a time range proportional to its penetration. The highest values for each section of analysis (area, crossings, and inflections) are highlighted in red and the lowest in green.

Antenna	Orientation	Range (ns)	Scan Area			Axis Crossings			Inflection Points		
			Clean	Mod. Clean	Mod. Fouled, Fouled	Clean	Mod. Clean	Mod. Fouled, Fouled	Clean	Mod. Clean	Mod. Fouled, Fouled
500 MHz	Perp.	10	809911	1019195	1073568	7.89	8.13	8.50	9.06	9.20	10.34
	Paral.	10	738316	916886	1461600	7.28	8.17	8.83	9.55	9.20	10.49
900 MHz	Perp.	5	249568	263324	274524	6.80	5.81	6.86	9.07	7.91	8.62
	Paral.	5	223292	258191	269580	6.40	5.60	6.52	8.96	7.37	8.28
1.0 GHz	Perp.	5	226772	249176	252872	7.03	7.04	7.13	8.45	8.06	7.87
	Paral.	5	939912	1178165	1172130	6.34	6.29	6.58	7.82	7.68	7.77
1.6 GHz	Perp.	3	386661	361702	353061	5.34	5.61	5.57	5.14	5.44	5.53
	Paral.	3	355258	412466	406161	4.91	4.59	4.52	4.89	4.94	4.92
2.6 GHz	Perp.	2	73915	80889	80193	1.00	1.00	1.00	0.49	0.39	0.39
	Paral.	2	93239	94230	95571	1.00	1.00	1.00	0.51	0.47	0.52

Table 6 Results of scattering analysis for proportional range

6.10 Proportional Range Scan Area Analysis

Akin to all the previously analysed time ranges, the clean ballast has a smaller area for the lower frequency antennas, but, yet again, this trend is not as clear as with the full time range results.

6.11 Proportional Range Axis Crossings Analysis

Although it appears that for most antennas the fouled ballast has a greater number of axis crossings, the numerical difference is not significant enough to demonstrate a clear trend.

6.12 Proportional Inflection Points Analysis

The trend in the results appears to be of a more random nature; although, the change in behaviour at 900MHz does still seem to be present.

7 METRIC EVALUATION

To evaluate the effectiveness of this method of measuring the scattering, the correlation between the scattering analysis for each crib and the fouling index for each crib was investigated.

Each area scan value for each crib was plotted against the measured fouling index for that crib and the trend line correlation value calculated. The best correlation was achieved with the 500MHz antenna using the full time range giving a correlation coefficient of 0.8 in the perpendicular orientation and 0.9 in the parallel orientation (Figure 15).
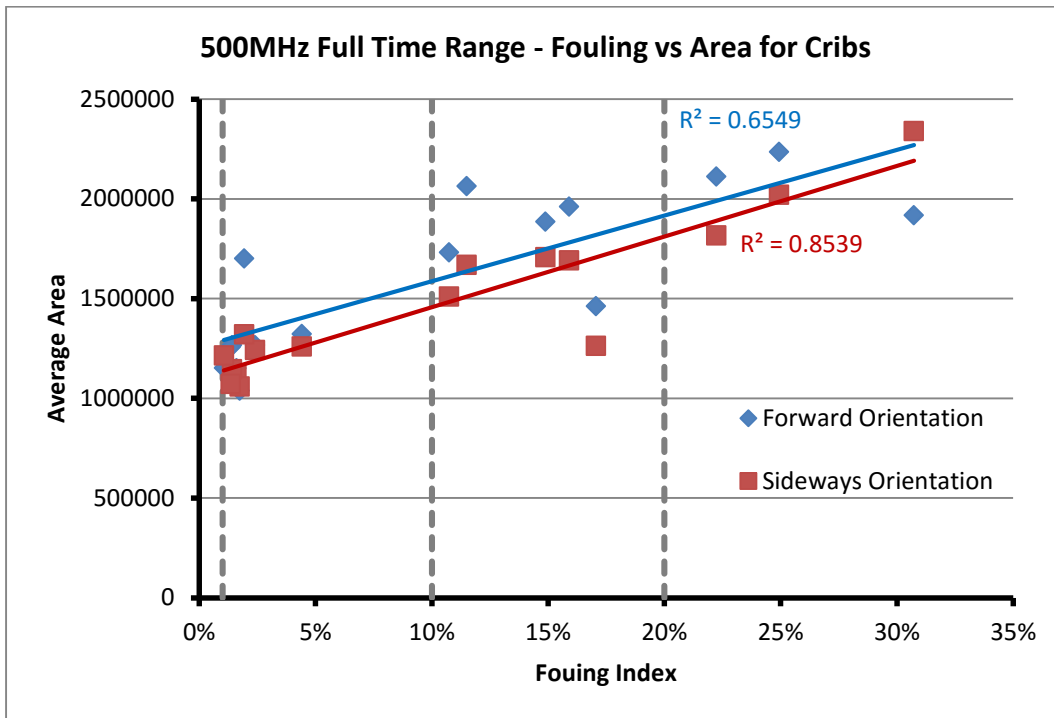
Figure 15 500MHz correlation analysis

The numerical correlation values for all experiments were also calculated (Table 7). Where the results correlated with a coefficient greater than 06, the text is light green; greater than 0.8, the cell is dark green; less than -0.6, yellow; less than -0.8, orange.

Antenna	Orientation	Scan Area			Axis Crossings			Inflection Points		
		Full Range	Com. Range	Prop. Range	Full Range	Com. Range	Prop. Range	Full Range	Com. Range	Prop. Range
500 MHz	**Perp.**	0.809	0.019	0.499	0.286	-0.356	0.378	0.462	0.616	0.619
	Paral.	0.924	0.566	0.816	0.295	0.674	0.613	0.034	0.133	0.213
900 MHz	**Perp.**	0.740	0.569	0.502	-0.599	-0.157	-0.074	-0.719	-0.488	-0.392
	Paral.	0.756	0.634	0.648	-0.439	0.076	0.041	-0.802	-0.289	-0.340
1.0 GHz	**Perp.**	0.436	0.519	0.519	-0.336	0.072	0.149	-0.481	-0.296	-0.423
	Paral.	0.678	0.641	0.679	-0.061	0.504	0.234	-0.340	-0.006	-0.057
1.6 GHz	**Perp.**	-0.185	-0.228	-0.257	-0.327	-0.388	0.180	-0.251	-0.079	0.448
	Paral.	0.545	0.672	0.676	-0.274	-0.466	-0.551	-0.221	-0.306	0.136
2.6 GHz	**Perp.**	0.282	0.111	0.722	-0.120	0.065	0.000	-0.647	-0.683	-0.563
	Paral.	0.326	0.342	0.301	-0.306	-0.140	0.000	-0.687	-0.721	0.035

Table 7 Fouling index correlation factors for full-time range scattering analysis

7.1 Scan Area Metric Evaluation

There was a strong correlation between the scan area metric and the fouling index for the full-time range. In order for the scan area metric to be true, the largest magnitudes of response should occur in the spent region of ballast.

For low frequency antennas scattering occurs more in spent ballast, correlating with Gallagher et al 1999 (Gallagher G. , Leiper, Williamson, Clark, & Forde, 1999). With higher frequency antennas, it is almost impossible to distinguish between clean and spent ballast in terms of scattering. This contradicts Al-Qadi et al (2008) who stated that with high frequency antennas more scattering occurs in clean ballast – however they used horn antennas.

The noticeably improved results in lower frequency antennas may be due to the increased power of the antenna itself - with the lower frequency antennas less likely to interpret minor changes in particle size and constituency as a change in material layer, which ultimately results in a better indication of ballast depth and layer interfaces.

7.2   Axis Crossings & Inflection Point Metric Evaluation

The axis crossings metric does not demonstrate any correlation in the data. The inflection point metric features a number of strong negative correlations, which mostly occur when the full-time range data is used. These results are less promising than data obtained from the scan area metric evaluation; however, the existence of some strong negative correlations suggests that there is a possible link between this scattering analysis and fouling index. In any case, both of these approaches are inappropriate for determining ballast fouling. It had been expected that when the range of data analysed was shortened to the depth of the ballast, i.e., 5ns, the correlation with the fouling index would improve. However, the opposite was true. It may be that the sub-ballast material gives a different response when under clean or spent ballast, and this may be due to drainage differences between clean and spent ballast.

8   CONCLUSIONS

An analysis of Fouling Indices (FI) concluded that the Ionescu FI was more appropriate for EU ballast, as the US Selig and Waters FI was based upon smaller size US ballast.

The full-time range results gave the most consistent results and strongest correlations. The results for this method are summarised below: -

Scan area	Clean ballast had the smallest area with most antennas; the spent or mixed ballast had the largest areas. The 500MHz antenna in the parallel orientation gave the best correlation (0.92) between fouling index and scan area.
Axis crossings	With antennas of 900MHz or over, clean ballast featured more axis crossings than the spent ballast. Below 900MHz, the behaviour reversed with the spent ballast having more axis crossings than the clean. There were no particularly strong correlations between fouling index and axis crossings.
Inflection points	With antennas of 900MHz or over, clean ballast featured more inflection points than the spent ballast. Below 900MHz, the behaviour reversed with the spent ballast having more inflection points than the clean. The 900MHz antenna in the parallel orientation gave the best correlation (-0.80) between fouling index and inflection points.

The overall conclusion is that GPR is a valuable investigative tool that can be used to determine the ballast fouling index (FI) using the Ionescu FI in conjunction with scan area metric evaluation procedure. A correlation coefficient greater than 0.9 was obtained by using a 500MHz bowtie antenna, in the parallel orientation, in conjunction with the scan area analysis.

9   ACKNOWLEDGMENTS

10 REFERENCES

Al-Qadi, I., Xie, W., & Roberts, R. (2008). Scattering analysis of ground-penetrating radar data to quantify railroad. *NDT&E International, 41*, 441– 447.

Al-Qadi, I., Xie, W., & Roberts, R. (2010). Optimization of antenna configuration in multiple-frequency ground penetrating radar system for railroad substructure assessment. *NDT & E International, 43*(1), 20-28.

Annan, A. P. (2008). Chapter 1 - Electromagnetic Principles of Ground Penetrating Radar. In H. Jol (Ed.), *Ground Penetrating Radar: Theory and Applications.* Elsevier Science & Technology Books.

Association of American Railroads. (2006). *Railroad Facts 2006.* Washington DC: Association of American Railroads.

Brough, M., Stirling, A., Ghataora, G., & Madelin, K. (2003). Evaluation of railway trackbed and formation: a case study. *NDT&E International, 36*, 145–156.

Bungey, J. H., & Millard, S. G. (1993). Radar inspection of structures. *Proceedings of the Institution of Civil Engineers: Structures and Buildings, 99*(2), 173-186.

Clark, M. (2001). *Non-Destructive and Geotechnical Testing or Railway Track Bed Ballast.* PhD thesis, University of Edinburgh.

Clark, M. R., Gillespie, R., Kemp, T., McCann, D. M., & Forde, M. C. (2001). Electromagnetic properties of railway ballast. *NDT&E International, 35*, 83-85.

Clark, M. R., Gordon, M. O., & Forde, M. C. (2004). Issues over high-speed non-invasive monitoring of railway trackbed. *NDT&E International, 37*(2), 131-139.

Daniels, D. J., Gunton, D. J., & Scott, H. F. (1988, August). Introduction to sub-surface radar. *Proceedings of Institution of Electrical Engineers, 135F*(4), pp. 278-320.

Dolphin, L. T., Beatty, W. B., & Tanzi, J. D. (1978). Radar Probing of Victorio Peak, New Mexico. *Geophysics, 43*(7), 1441-1448.

Forde, M. C., & McCavitt, N. (1993). Impulse radar testing of structures. *Proceedings of the Institution of Civil Engineers: Structures and Buildings, 99*(1), 96-99.

Gallagher, G. P. (1999). *Investigation of Railway Trackbed Deterioration using Ground Penetrating Radar.* MSc Thesis, University of Edinburgh.

Gallagher, G. P., Leiper, Q., Clark, M., & Forde, M. C. (2000, February). Ballast evaluation using ground penetrating radar. *Railway Gazette International*, pp. 101-102.

Gallagher, G., Leiper, Q., Williamson, R., Clark, M., & Forde, M. (1999). The application of time domain ground penetrating radar to evaluate railway track ballast. *NDT&E International, 32*(8), 463-468.

Hugenschmidt, J. (1999). Ballast inspection using ground penetrating radar. *Proceedings of the Second International Conference on Railway Engineering.* London: Engineering Technics Press, Brunel University.

Hugenschmidt, J. (2000). Railway track inspection using GPR. *Journal of Applied Geophysics, 43*, 147-155.

International Union of Railways. (2011). UIC world rail statistics for 2010. *Press release*.

Ionescu, D. (2004). Ballast degradation and measurement of ballast fouling. *Proceedings of 7th International Railway Engineering Conference.* London: Engineering Technics Press.

Jack, R., & Jackson, P. (1998). Imaging attributes of railway track formation using ground probing radar (GPR). *Proceedings of the First International Conference on Maintenance and Renewal of Permanent Way and Structures.* London: Engineering Technics Press, Brunel University.

Parker, S. P. (1997). *Dictionary of Engineering* (5th Edition ed.). McGraw-Hill.

Roberts, R., Al-Qadi, I., Tutumluer, E., Boyle, J., & Rudy, J. (2006). Railroad Ballast Fouling Detection Using Ground Penetrating Radar – A New Approach Based on Scattering from Voids. *Ninth European Conference on NDT.* Berlin.

Roberts, R., Al-Qadi, I., Tutumluer, E., Boyle, J., & Sussmann, T. (2006). Advances in Railroad Ballast Evaluation Using 2GHz Horn Antennas. *11th International Conference on Ground Penetrating Radar.* Columbus.

Selig, E. T., & Waters, J. M. (1994). Track Geotechnology and Substructure Management. Thomas Telford.

Sharpe, P. (2000). Trackbed investigation. *Journal and report of proceedings - Permanent Way Institution, 118*(3), 238-254.

Sharpe, P., & Collop, A. C. (1998). Trackbed investigation - a modern approach. *Proceedings of the First International Conference on Maintenance and Renewal of Permanent Way and Structures.* London: Engineering Technics Press, Brunel University.

Soutsos, M. N., Bungey, J. H., Millard, S. G., Shaw, M. R., & Patterson, A. (2001). Dielectric properties of concrete and their influence on radar testing. *NDT & E International, 34*(6), 419-425.

Sussmann, T. R. (1999). *Application of Ground Penetrating Radar to Railway Track Substructure Maintenance Management.* PhD thesis, University of Massachusetts Amherst.

UK Department of Statistics. (2007). *Transport Trends: 2007 Edition - Section 3: Public Transport, Trend 3.4b - Distance travelled by National Rail passengers: 1980 to 2006/07*. Retrieved September 18, 2008, from http://www.dft.gov.uk/162259/162469/221412/190425/220778/trends2007

UK Department of Transport. (2013). *Rail Passenger Miles.* Retrieved March 3, 2014, from Gov.UK: https://www.gov.uk/government/publications/rail-passenger-miles

Zarembski, A. M. (1988). Performance Characteristics for Concrete Tie Fasteners. *Rail International*.